Reasons for drop in shell-and-tube condenser performance when replacing R22 with R407C

Dave Sajjan and Lennart Vamling

Department of Heat and Power Technology,
Chalmers University of Technology, SE-412 96 Göteborg, Sweden
Dave.sajjan@hpt.chalmers.se and lennart.vamling@hpt.chalmers.se

Abstract—An experimental and theoretical investigation was made to find out the reasons for the drop in shell-and-tube condenser performance when replacing R22 with a zeotropic mixture R407C. Measurements have shown that at lower condenser loads the performance drop can be as large as 75% compared to the full condenser load. Computed results are compared with both previous data and experimental results. Computed results show that the degree of mixing of the newly formed and the drained condensate is a factor influential enough to explain the performance drop. About 10% more condensation area is needed due to mass transfer resistance.

Introduction

Since no single fluid meets all the economic, environmental and non-toxic criteria as a replacement for R22, blends of different substances are under consideration. One such mixture is R407C (38% by mole R32, 18% R125 and 44% R132a). Experimental results after such a replacement show, however, in some applications, a severe drop in condenser performance [1]. This drop can be as large as 70% compared to R22 at low effects. In [1], several possible reasons for the drop were investigated, but no single factor explaining it was found. Here, additional reasons will be investigated. A comprehensive steady-state model describing condensation of the multi-component mixture R407C in a shell-and-tube type condenser is developed to accomplish this.

Condensation of a vapour mixture differs from that of a pure fluid in only two ways: the temperature, at which condensation occurs, changes throughout the condenser, and the effects of mass transfer resistance are introduced. As the heavier components are more liable to condense first, the remaining mixture has a lower dew temperature, thus causing the equilibrium temperature to fall. The practical significance of such a temperature fall will be reduced temperature difference between the condensate and the coolant with a corresponding reduction in local heat transfer. Also the preferential condensation of the heavier component leads to accumulation of the lighter components

at the condensate-gas interface, thus making a film through which the heavier components have to diffuse. Since the condensation is not isothermal, there are liquid-phase sensible effects present as well as gas-phase sensible effects.

Since the local thermodynamic parameters (condensation temperature, latent heat etc.) are directly related to the local vapour and condensate compositions, the relative paths of the vapour and the condensate, in the case of mixtures with glide, need to be known. Depending on the mixing in the condensate layer, the condensation of mixtures with temperature glide can be classified using two extremes: differential and integral condensation.

Differential condensation occurs when draining condensate from the tubes situated above does not influence the concentration in the condensate at the gas-condensate interface. The possible reasons may be one or the other of the following:

1. Condensate segregation or condensate holdup.
2. Different flow paths of the gas and the condensate.
3. Infinite mass transfer resistance.

The other extreme, integral condensation, occurs when there is perfect mixing between new and old condensates.

To avoid the differential kind of condensation, condensation on the tube side in the case of a zeotropic mixture is preferable. In many applications, however, the coolant (water) side is subject to fouling. Due to practical problems of cleaning on the shell side in such cases, condensation on the shell side is common.

In the present work, a model is developed for the analysis of a shell-and-tube type condenser for multi-component mixtures. Results from simulations are compared to experimental results obtained from a full-scale experimental facility.

Theoretical Modelling

The model describes the condensation of a refrigerant mixture that can be saturated or superheated at the inlet. The condenser under consideration is of TEMA X type with cross-flow arrangement and two tube-side passes. The vapour condenses on the shell side of the tubes, forming a condensate layer. The vapour phase is assumed to be fully mixed and the condensate formed on a tube row is assumed to spread equally over the tubes on the subsequent row. Mass transfer due to temperature gradients is ignored.

Figure 1 illustrates the heat and mass transfer processes around a tube in a tube bank. A heat balance over the tube cross-section can be written as:

$$dQ_L = dq_g + dq_L + N_{tot} \cdot h_{fg} \cdot M_m \qquad \textbf{(1)}$$

where dQ_L is the heat conducted from the gas-liquid interface to the coolant, and the terms on the right-hand side of the equation are the sensible heat dq_g removed from the gas bulk, the sensible heat dq_L extracted from the condensate falling from the tube above, and the latent heat h_{fg} of the condensing vapour flux N_{tot}.

In order to calculate the condensing mass flux N_{tot}, Stefan & Maxwell's equations for the multi-component gas mixture are solved, assuming that the gas mixture behaves as an ideal gas. Stefan & Maxwell's equations under isothermal and isobaric conditions for a mixture of **K** components can be written as

$$\frac{dy_i}{dz} = \sum_{\substack{j=1 \\ j \neq i}}^{K} \frac{y_i N_j - y_j N_i}{C D_{ij}} \qquad i = [1,\mathrm{K}-1] \qquad \textbf{(2)}$$

where N_i are the molar fluxes toward the condensate surface and D_{ij} is the binary diffusion coefficient of component *i* in component *j*. These coefficients are estimated from [2]. If δ is the gas film thickness, a dimensionless distance coordinate $\eta = z/\delta$ yields

$$\frac{dy_i}{d\eta} = \sum_{\substack{j=1 \\ j \neq i}}^{K} \frac{y_i N_j - y_j N_i}{\beta_{ij}} \qquad i = [1,\mathrm{K}-1] \qquad \textbf{(3)}$$

where k_{ij} (mol/m^{2}s) are binary mass transfer coefficients and

$$\beta_{ij} = C \frac{D_{ij}}{\delta}$$

where C is the gas molar density $C = \frac{p}{RT}$. If we assume that the transition between the bulk molar fraction y_b and the interface molar fraction $\mathbf{y}_I$ takes place in the stagnant gas film of thickness δ and that the analogy between heat and mass transfer [3] is valid, i.e.

$$j_h = \frac{h_g}{Cp_g} \mathrm{Pr}^{2/3} = j_D = \beta_{ij} Sc^{2/3} \qquad \textbf{(4)}$$

then the binary mass transfer coefficients $\beta_{g,ij}$ for each species pair can be calculated after inserting the expressions for Pr and Sc numbers:

$$\beta_{g,ij} = \frac{h_g}{Cp_g}\left(\frac{CD_{ij}Cp_g}{k_g}\right)^{2/3} \quad \textbf{(5)}$$

where h_g is the gas-phase heat transfer coefficient taken from [22], Cp_g is the heat capacity of the gas mixture and k_g is the gas conductivity. All the physical properties in equation (5) are taken at the gas-bulk temperature, pressure and composition.

Krishna and Standart [4] have developed a mathematical procedure to solve Stefan-Maxwell's equations. The system of equations (3) can, according to [4], be solved for condensing mass fluxes if the concentration gradients (i.e. $dy_i/d\eta$) in the gas film are known.

It is assumed that the gas phase and the condensate at the interface are in thermodynamic equilibrium. Since the heavier components are more liable to condense first, the equilibrium temperature at the subsequent row will depend upon the composition of the condensate at that tube row. If the condensate from the first tube row leaves the system, the equilibrium will exist between the gas enriched with lighter component and the condensate formed from it. The other extreme will occur, if the condensate from the upper tube mixes with the newly formed condensate so that the composition of the system remains constant. To model the above-mentioned phenomena, a mixing parameter ϕ is introduced in this work that varies between zero and unity. When ϕ is equal to unity, the condensation is integral, meaning that drained condensate and the condensate formed on the actual tube are well mixed. When ϕ is zero, no condensate mixing takes place. The fraction of component *i* in the condensate at the interface can be written as

$$x_{iI} = \phi x_i^{\text{int}} + (1-\phi)x_i^{diff} \quad \textbf{(6)}$$

where x_i^{int} is the molar fraction of the component *i* in the condensate when the drained condensate and the condensate formed on the tube under consideration are completely mixed, and x_i^{diff} is the molar fraction when no mixing in the condensate layer takes place, i.e.

$$x_i^{diff} = \frac{N_i}{\sum_{i=1}^{K} N_i}$$

where N_i is the condensing molar flux of component *i*.

If the pressure is known, the vapour-phase molar fraction and the interface temperature can be calculated from thermodynamic equilibrium:

$$(y_I, T_I) = f(x_I, p) \quad \textbf{(7)}$$

where y_I , x_I are the vectors of molar fractions of the components in the gas phase and in the condensate respectively.

If the gas is superheated, the sensible heat transferred from the gas bulk to the interface can be written as

$$q_g = h_g^{\bullet}(T_b - T_I) \quad \textbf{(8)}$$

where $h_g^{\bullet}$ is the gas-phase heat transfer coefficient corrected for the mass transfer effects. This correction is needed since the heat flux arrives at the interface as sensible heat arises from two sources: the cooling of the main gas stream, and the cooling of the condensing mass fluxes N_i from the bulk-gas temperature T_b to the interface temperature T_I. The coefficient $h_g^{\bullet}$ can be calculated, as pointed out in [5, 6]:

$$h_g^{\bullet} = h_g \frac{\theta}{1 - e^{-\theta}} \quad \textbf{(9)}$$

where

$$\theta = \frac{\sum_i N_i Cp_i}{h_g}$$

where Cp_i is the partial molar heat capacity for component *i*.

Now the temperature change in the main bulk gas stream can be written as

$$(G / M_m) Cp_m \frac{dT_b}{dA_o} = -q_g + \sum_{i=1}^{K} N_i Cp_i (T_b - T_I) \quad \textbf{(10)}$$

where G is the mass flow of the mean gas stream and dT_b is change in bulk gas temperature. Equations (8, 9 and 10) give

$$(G / M_m) Cp_m \frac{dT_b}{dA_o} = h_g \frac{\theta}{e^{\theta} - 1}(T_b - T_I) \quad \textbf{(11)}$$

The latent heat of the condensing vapour together with sensible heat from the bulk gas is transferred from the gas-condensate interface to the coolant by conduction:

$$dQ_L = h_L(T_I - T_c)dA_o = (m_c / M_c)Cp_c\Delta T_c \qquad \textbf{(12)}$$

where h_L indicates the heat transfer coefficient from the condensate surface to the coolant, dA_o is the surface area element of the interface, T_I its temperature, T_c the local temperature of the coolant and m_c the coolant flow rate (kg/s).

The heat transfer coefficient h_L can be written as

$$\frac{1}{h_L dA_o} = \frac{1}{h_l dA_o} + \frac{R_s}{dA_o} + \frac{\delta_w}{\lambda_w dA_w} + \frac{R_t}{dA_t} + \frac{1}{h_c dA_t} \qquad \textbf{(13)}$$

where h_l represents the heat transfer coefficient of the condensate film, R_s the fouling on the shell side or the condensate side, δ_w the thickness of the wall, λ_w the wall thermal conductivity, R_t the fouling on the coolant side or the tube side, dA_t the surface area element on the cooling surface, and h_c the heat transfer coefficient on the coolant side, which is calculated from Ditteus & Boelter's equation.

The heat transfer coefficient for the condensate film in a bundle of finned horizontal tubes is subject to the combined effects of condensate inundation, vapour shear, condensate retention, the tube arrangement and the shape of the fins. If the effect of vapour shear is insignificant and condensate drains only due to gravity, the heat transfer coefficient for a horizontal plane tube can be calculated according to Nusselt [7]:

$$\bar{h}_l = 0.725\left(\frac{k_l^3 \rho_l^2 g h_{fg}}{\mu_l}\right)^{1/4}\left(\frac{1}{(T_i - T_w)}\right)^{1/4}\left(\frac{1}{d_r}\right)^{1/4} \qquad \textbf{(14)}$$

where d_r is the plane-tube diameter. Using a heat balance over the tube, the above equation can be written as

$$\frac{\bar{h}_l}{k_l}\left[\frac{\mu_l^2}{\rho_l(\rho_l - \rho_g)g}\right] = 1.51\left(\frac{4\Gamma}{\mu_l}\right)^{-\frac{1}{3}} \qquad \textbf{(15)}$$

where Γ is the mass flow rate of the condensate per unit length of the tube (kg/m$\cdot$s).

To enhance the heat transfer for the refrigerants with low conductivity and latent heat, finned tubes are commonly used. Finned tubes provide not only increased heat transfer area per unit tube length, but also increased heat transfer due to vertical fin flanks having higher condensation heat transfer coefficients than that for the tube base [8]. A theoretical model for the calculation of the heat transfer coefficient on finned tubes was proposed by Beatty and Katz [9]. In this model, the effect of surface tension was neglected, and condensation was considered only gravity-driven. A number of groups [9, 10, 11, 12, 13, 14] have studied the performance of Beatty and Katz [9] model. However, [14, 11, 13] have observed that the model overpredicts or underpredicts the

heat transfer performance depending on the fluid and geometry of fins. It underpredicts condensation on fin flanks and overpredicts the active surface area. Error increases at higher fin density and for fluids having higher surface tension.

The model of Beatty and Katz [9] for the heat transfer coefficient on finned tubes is based on adding up the contributions of the fin flanks and the tube surface between the fins:

$$h_l = h_u \frac{A_r}{A_o} + \eta_f h_f \frac{A_f}{A_o} \qquad \textbf{(16)}$$

where η_f represents the fin efficiency and A_o is the effective area, i.e. the sum of the areas of the fins A_f and the bare tube A_u, while h_u is the Nusselt coefficient for horizontal tubes and h_f stands for the Nusselt coefficient for a vertical plate:

$$h_u = 0.725\left(\frac{k_l^3 \rho_l^2 g h_{fg}}{\mu_l (T_I - T_w) d_r}\right)^{1/4} \qquad \textbf{(17)}$$

$$h_f = 0.943\left(\frac{k_l^3 \rho_l^2 g h_{fg}}{\mu_l (T_I - T_w) H_f}\right)^{1/4} \qquad \textbf{(18)}$$

After inserting the expressions for h_t and h_f, they arrived at

$$h_l = 0.689\left[\frac{k_l^3 \rho_l^2 g h_{fg}}{\mu_l (T_I - T_w) d_{eq}}\right]^{1/4} \qquad \textbf{(29)}$$

where d_{eq} is an equivalent diameter given by

$$\left\{\frac{1}{d_{eq}}\right\}^{1/4} = \frac{0.943}{0.725}\eta_f \frac{A_f}{A_o}\frac{1}{H_f^{1/4}} + \frac{A_u}{A_o}\frac{1}{d_r^{1/4}} \qquad \textbf{(20)}$$

where H_f is the mean effective height of a fin:

$$H_f = \frac{\pi}{4 d_f}(d_f^2 - d_r^2)$$

The adjustment of the theoretical value 0.725 in equation (14) to 0.689 correlated their experimental data within ±10%.

Using a heat balance over the tube, equation (19) can be written as

$$h_l = 0.645\left(\frac{1}{d_{eq}}\right)^{1/3}(A_o)^{1/3}\bar{h}_l \qquad \textbf{(21)}$$

where $\bar{h}_l$ is given by equation (15). Equation (21) gives the heat transfer coefficient when there is no condensate inundation, i.e. for the top tube in a tube bundle. Heat transfer coefficients along a tube bundle are generally expressed as $h_N/h_1 = f(N)$, where N is the tube-row number and h_N and h_1 are the condensation heat transfer coefficients for the N^{th} and for the first row respectively. Various authors [10, 15, 16] have studied the effects of condensate inundation in tube banks. According to Blanc et al. [10], the effects of inundation on the type of tubes used in this work can be best described with the expression proposed by Kern [16]:

$$h_{lN} = h_{l1}(N)^{-1/6} \qquad \textbf{(22)}$$

where h_{l1} is the heat transfer coefficient for the top row. According to Butterworth [17], equation (22) is in close agreement with the equation proposed by Grant and Osment [18] and used in the present work:

$$h_{lN} = h_{l1}\left\{\frac{\Gamma_N}{\gamma_N}\right\}^{-0.223} \qquad \textbf{(23)}$$

where Γ_N is the condensate drainage from the N^{th} tube and γ_N is the condensate formed at that tube.

Calculation Procedure and the Computer Program

The condenser area is divided into a number of computational cells. The tube length is divided into slices. A cell consists of the area spanned by a slice and a tube row. For the given temperature, pressure and mass flow of the vapour and the coolant at the cell inlet, the gas flow, temperature and pressure at the outlet are obtained by solving the mass and heat transfer equations, by using a forward differencing scheme.

The gas flow is divided equally to all slices in the top tube row. After each tube row an average value of the gas flow and concentration is calculated and is divided equally to all slices in the next tube row. In this way, a varying number of tubes per tube row can be handled.

The heat transfer coefficient for the gas bulk is calculated by using a one-phase correlation with physical properties taken at average temperature and pressure. The average flow rate around each tube row is calculated from the total gas flow and the available gas flow area. Note that this available flow area includes the bypass area between the shell and the tube bank.

For the condenser under consideration, there are two tube-side passes and the rise in coolant temperature is calculated from equation (12). An average temperature of the coolant from the first pass is the inlet temperature to the second pass.

If the area needed for condensation is not equal to the area available, then the heat transfer coefficient h_l (equation (14)) is multiplied by an error factor. This factor can be greater than one if the area required is higher than the available area, or vice versa. A global value for the correction factor ε (see further sections) is calculated from the program.

The overall calculation scheme is:

1. Read the input data and geometry files.
2. Assume $\varepsilon = 1$.
3. Tube passes:
   3.1 If one pass, then inlet coolant temperature to all tube rows = inlet coolant temperature.
   3.2 If two passes, then assume inlet coolant water temperature to the upper half of the tube rows and the lower half of the tube rows has the same temperature as the coolant.
4. Do, For Tube rows = 1 to Number of tube rows:
   4.1 Calculate zero-flux mass transfer coefficient and physical properties at the bulk gas-phase conditions
      4.1.1 Do, For slices = 1 to Number of slices:
         4.1.1.1 Assume molar fluxes N_i.
         4.1.1.2 Calculate mass transport resistance coefficient ξ [4]
         4.1.1.3 Calculate condensate molar fraction x_i for a given ϕ (eq. 6) and for the top tube row when ϕ is equal to zero.
         4.1.1.4 Using conditions of thermodynamic equilibrium, calculate interface molar fraction for the gas phase (eq. 7).
         4.1.1.5 Use heat balance (eq. 1) to calculate the total condensing mass flux to the interface.
         4.1.1.6 If the difference between the assumed and the calculated N_i is not less than the specified error, then go to step 4.1.1.1 with calculated values of N_i.
      4.1.2 Calculate the bulk gas temperature (eq. 12) and coolant temperature (eq. 13).
      4.1.3 Calculate average bulk gas flow, temperature, composition and pressure drop.

5. Calculate average coolant temperature.
6. If one tube-side pass, calculate the average temperature and go to step 7.
   6.1 If two tube-side passes:
      6.1.1 Calculate the average outlet temperature from the second pass and if (calculated – assumed in step 1.2) > ε, then iterate, otherwise continue to step 7.
7. If $A_{calc} \neq A$ then $\varepsilon = \varepsilon_{new}$ and go to step 2.
8. If all the available area is used, Stop and write data to an output file.

Experimental apparatus

The condenser under consideration is of TEMA-X type with two tube-side passes, where condensation takes place on the shell side of low-3D-fin tubes.

The total shell-side surface area for the condenser under consideration is around 320 m^2. The volume flow and in-and-out temperature of the coolant are measured. The same instrumentation is available for the refrigerant side except that the mass flow of the working fluid is calculated from an energy balance. The gas pressure is measured at the condenser inlet. A more detailed description of the experimental rig is given in [1]. Note here that the condensers in [1] and in the present work are different.

The tests were carried out under the same conditions as the chiller was constructed for. In order to vary the heat flux without changing the condensation temperature, the refrigerant mass flow was adjusted by varying the compressor capacity by adjusting the number of revolutions.

Results and Discussion

The overall heat transfer coefficient (U) can be used to compare the performance of a condenser, and is generally expressed as

$$U = \frac{Q}{A\Delta\overline{T}} \qquad \textbf{(24)}$$

where A is the total heat transfer area, $\Delta\overline{T}$ is an average temperature driving force, and Q is the total transferred effect. The measured overall heat transfer coefficient is calculated by using

$$\Delta\overline{T}_{\ln} = \frac{(\Delta T_{\ln,cc} + \Delta T_{\ln,co})}{2} \qquad \textbf{(25)}$$

as the temperature driving force, where

$$\Delta T_{\ln,cc} = \frac{(T_{b,in} - T_{c,out}) - (T_{b,out} - T_{c,in})}{\ln \dfrac{(T_{b,in} - T_{c,out})}{(T_{b,out} - T_{c,in})}} \qquad \textbf{(26)}$$

and

$$\Delta T_{\ln,co} = \frac{(T_{b,in} - T_{c,in}) - (T_{b,ut} - T_{c,ut})}{\ln \dfrac{(T_{b,in} - T_{c,in})}{(T_{b,ut} - T_{c,ut})}} \qquad \textbf{(27)}$$

are the log mean temperature differences for the co-current and the counter-current flow, respectively.

The overall heat transfer coefficient from the simulations, U_{calc}, is obtained by calculating the average temperature driving force as

$$\Delta \overline{T} = \frac{1}{\int_0^Q \left[\dfrac{dq/Q}{\Delta T_{\ln}} \right]_{dA_o}} \qquad \textbf{(28)}$$

where ΔT_{ln} is calculated by using equations (25, 26 and 27) in each cell.

Note, however, that the overall value of U_{meas} refers to the total condenser area and U_{calc}, the calculated overall heat transfer coefficient, refers to the area required for total condensation. The comparison of U_{meas} and U_{calc} can be misleading since these are based on different areas. Even if U_{calc} is corrected by multiplying with A_{calc}/A, the comparison is not based on the same temperature driving force. One alternative is to multiply the locally calculated h_L with an error factor ε. This error factor is then adjusted to obtain the same outlet conditions as found experimentally.

Experimental Results

A summary of the experimental results is given in Table 1. As can be seen, the tests were performed for different inlet coolant temperatures and compressor capacities.

Table 1: Summary of Experimental Runs.

Case No.	Gas Temp. (°C)	Gas Pressure (bar)	Coolant in-Temp. (°C)	Coolant flow (kg/s)	Effect (kW)
1	66.2	16.58	32.37	48.8	1156
2	66.3	16.55	32.36	48.5	1138
3	66.7	16.54	32.36	48.8	1138
4	56.4	13.1	22.55	49	1119
5	61.6	14.58	27.53	49	1050
6	65.1	16.31	32.36	49	1007
7	68.1	13.80	27.49	49	691
8	62.4	15.42	32.3	49	457
9	72.5	13.62	28.53	50	445
10	63.0	13.43	26.42	49	359
11	73.4	13.77	29.52	50	170
12	73.1	13.65	29.00	50	162
13	69.8	14.47	29.43	50	139
14	67.8	14.44	29.55	50	129
15	66.8	14.27	29.56	50	128

Simulation results

Comparison with literature data

The present model was validated against the experimental data for pure R22 and R407C presented in [1]. The results are presented in Fig. 2 in terms of correction factors when the condensation curve is assumed to be integral, i.e. ϕ=1. As shown, the present model overpredicts the liquid overall heat transfer coefficient (h_L) by ≈14% for R22 when the effect varies between 750 kW and 250 kW. However, the overprediction in the case of R407C varies between 40% at high condensation rates and 65% at low condensation rates.

Now the question is, what are the possible reasons for the different behaviour of R407C and R22. Both R407C and R22 have very similar thermophysical properties except that R407C is a zeotropic mixture, which means that the local condensation temperature will depend upon the composition of the condensate at the gas-condensate interface. Calculations were made to find the degree of mixing in the condensate layer, i.e. for different ϕ to obtain the correction factor equal to the correction factor for R22. The resulting integration ratios are plotted against the effect in Fig. 3.

From this, we can see that the mixing pattern in the liquid or the condensate phase is a factor influential enough to explain the difference in condensation rate between the pure fluid and the mixture in this condenser. It also seems that there is less mixing at higher effects. As shown in the figure, the integration ratio is equal to 0.23 when the effect is 735 kW and around 0.64 when the effect is 250 kW. The thicker condensate layer at higher condenser effects might explain this but, on the other hand, there could be more turbulence in the layer. More local measurements in tube banks are needed to determine which of the above two effects dominate.

Comparison with experimental data

The overall heat transfer coefficient U_{meas} obtained from equations (24, 25, 26 and 27) and the calculated U_{calc} corrected with area ratio A_{calc}/A are shown in Fig. 4. As mentioned before, even though the U_{calc} presented in Fig. 4 is corrected with the area ratio in order to define it for the total condenser area, the temperature driving force is not the same as in the experimental case. It will be more logical to compare the model results in terms of correction factor. Figure 5 presents the comparison in terms of correction factor. As we see, for this condenser with different geometrical parameters than the one considered in [1], model predictions are very close to the experimental data when the condenser effect is between 100 and 70% of the maximum condenser effect. However, at lower effect, less than 30% of the maximum effect, the model overpredicts the heat transfer performance.

Figure 5 illustrates the integration ratio, i.e. the degree of mixing in the condensate layer needed to get the same outlet conditions as in experiments. As can be seen, at low effects the model predicts the same outlet conditions as in experiments for a value of integration ratio ≈ 0.80. It indicates that mixing in the condensate layer for the kind of tubes used in the present work is better than for the tubes used in [1].

Effect of mass transfer resistance

The sweeping of the lighter components to the interface by the condensing flux results in a higher concentration of the lighter components at the interface, and hence provides resistance to the mass transport of the heavier components. The higher concentration of the lighter components results in lower interface temperature, which means reduced temperature-driving force or increased area requirement.

The effect of mass transfer resistance was investigated by varying the values of diffusion coefficients since this effect should be negligible at very high diffusion coefficients. The comparison is made by comparing the area needed for condensation for case 11, Table 1, and assuming $\phi=1$. The diffusion coefficients were varied as in Table 2, whose bold **D** is a matrix of the diffusion coefficients estimated from [2]. As

we see, when the diffusion coefficients are 8 to 16 times the estimated diffusion coefficients, the area needed for condensation to the total area is almost constant, which means 10% more area is needed due to mass transfer resistance.

Table 2: Summary of Results for Mass Transfer Resistance

Diffusion coefficient [m^2/s]	Area Needed /Total Area
0.25 ***D**	0.68
0.5 ***D**	0.57
1 ***D**	0.52
2 ***D**	0.47
4 ***D**	0.46
8 ***D**	0.42
16***D**	0.42

Uncertainties and the Additional Factors

The present model assumes that the velocity and the concentrations of the components are uniform across a tube row and that the flow of gas mixture and condensate is vertical downward. A more correct method would be to solve the forced convected and diffusional flow patterns across the tube bank. In a coming article, a more detailed condenser model using Computational Fluid Dynamics (CFD) will be presented.

In the present work a parameter was introduced to represent the mixing in the condensate layer to obtain the compositions at the gas-condensate interface. The mixing parameter or integration ratio (ϕ) should, however, depend upon the local condensate loads and the local condensation rates. To get local integration factors, the mass diffusion in the condensate layer needs to be solved.

Liquid flow patterns may not be equally spread as assumed in the present model. The model of Beatty and Katz [9], originally developed for 2-D fins, is used to estimate the heat transfer coefficient for 3-D finned tubes used in the present case.

Conclusions

A structural framework for the analysis of condensers for multi-component mixtures, superheated or saturated, has been developed in a form suitable for computer use. The model takes into account the effects of mass transfer resistance and the mixing in the condensate layer. Since the pure experimental fluid for the condenser considered in the present work was not available, the model was validated against the existing data [1].

From the above discussion and the obtained results, the following conclusions can be drawn.

The degree of mixing in the condensate layer is a factor influential enough to explain the decrease of condenser performance found when replacing R22 with R407C in an earlier work.

Higher values of the mixing factor ϕ for 3-D finned tubes show that mixing in the condensate layer is better for 3-D finned tubes than for integral finned tubes. 10% more condensation area is required due to mass transfer resistance.

Acknowledgements

We wish to thank Sabroe Refrigeration AB for collaboration and for providing the experimental data, and the Swedish National Board for Industrial and Technical Development, NUTEK, for financial support.

Table of Nomenclature

A_o	outside surface area of tube (m^2/m)
A_f	surface area of fins (m^2/m)
A_r	surface area of tube with fin-root diameter (m^2/m)
A_t	inside surface area of tube (m^2/m)
C	molar density (mol/m^3)
Cp	heat capacity (J/mol k)
d_{eq}	equivalent diameter (m)
d_f	diameter to the outside of fin tips (m)
d_r	diameter to the fin roots (m)
D_{ij}	diffusion coefficient of component *i* in *i*
e	base of natural logarithms, 2.718…..
g	gravitational acceleration (m/s^2)
G	gas flow (kg/ m^2s)
H_f	fin height (m)
h_{fg}	specific enthalpy of vaporization (J/kg)
h_g	heat transfer coefficient for the gas film (W/m^2K)
h_c	heat transfer coefficient on the coolant side (W/m^2K)
h_l	heat transfer coefficient for the condensate film (W/m^2K)
h_L	heat transfer coefficient from interface to the coolant(W/ m^2K)
j	heat and mass transfer factor (equation 4)
k	thermal conductivity (W/mK)

M_m mean molar weight of the mixture (kg/mol)
M_c molar weight of the coolant (kg/mol)
m_c coolant mass flow rate (kg/s)
N tube number in tube-bank
N_i molar flux of component *i* towards the interface (mol/m^2s)
N_{tot} total molar flux (mol/m^2s)
p total pressure (Pa)
q_L heat flux from the interface to the coolant (W/m^2)
q_g heat flux from the bulk gas to the interface (W/m^2)
Q total condenser effect (W)
R molar gas constant (J/mol K)
R_t,R_s fouling resistance on tube and shell side (m^2K/W)
T_c coolant temperature (K)
T_b bulk gas temperature (K)
T_I interface temperature (K)
U overall heat transfer coefficient with respect to total outer surface area (W/m^2K)
$\mathbf{x_I}$ vector of molar fraction of components in condensate at the interface
y_b mole fraction of component *i* in the bulk gas
$\mathbf{y_I}$ vector of gas-phase molar fraction of components at the interface
z coordinate direction
λ_w wall thermal conductivity (W/mK)
δ gas film thickness (m)
δ_w tube wall thickness (m)
ϕ integration ratio or the degree of mixing in the condensate layer
κ_{ij} mass transfer coefficient (mol/ m^2s)
μ dynamic viscosity (kg/ms)
ρ density (kg/m^3)
ρ

Superscripts and subscripts
C coolant
calc calculated
diff no condensate mixing takes place
g gas phase
i component *i* in the mixture
l condensate
int when condensate is assumed to be completely mixed
sim simulated
meas measured

References

1. Gabrielii, C., Vamling, L., “Replacement of R22 in shell-and-tube condensers: Experiments and simulations”, International Journal of Refrigeration,1997, Vol. 20, pp. 165-178.
2. Fuller, E.N., Schettler, P.D., Giddings, J.C., “A New Method For Prediction Of Binary Gas-Phase Diffusion Coefficients”, Industrial and Engineering Chemistry, 1966, Vol. 58, No. 5, pp. 19-27.
3. Chilton T.H., Colburn, A.P., “Mass Transfer (Absorption) Coefficients, prediction from data on Heat Transfer and Fluid Friction”, Industrial and Engineering Chemistry, 1934, Vol. 16, No. 11, pp. 1183-1187.
4. Krishna, R., Standart, G.L., “A Multicomponent Film Model Incorporating a General Matrix Method of Solution to the Maxwell-Stefan Equations”, AIChE Journal, 1976, Vol. 2, No. 2, pp. 383-389.
5. G. Ackermann, “Forschungsheft”, 1934, No. 382, pp. 1-16.
6. Colburn, A.P., Drew, T.B., ”The Condensation of Mixed Vapors”, AIChE, 1937, Vol. 33, pp. 197-214.
7. Nusselt, W., “Die Oberflachen-Kondensation des Wasserdampfes”, 1916, VDI Zeitung, Vol. 60, 541-546, 569-575.
8. Briggs, A., Rose, J.W., “Condensation Performance of Some Commercial Integral Fin Tubes With Steam and CFC113”, Experimental Heat Transfer, 1995, Vol. 8, pp. 131-143.
9. Beatty, K.O., and Katz, D.L., “Condensation of vapors on outside of finned tubes” Chem. Eng. Prog., 1948, Vol. 44, pp. 55-70.
10. Blanc, Ph., Bontemps, A., Marvillet, Ch., “Condensation Heat Transfer of HCFC22 and HFC134a Outside a Bundle of Horizontal Low Finned Tubes”
11. Honda, H., Uchima, B., Nozu, S., Nakata, H., Torigoe, E., “Film Condensation of R-113on Inline Bundles of Horizontal Finned Tubes”, Journal of Heat Transfer, 1991, Vol. 113, pp. 479-486.
12. Honda, H., Nozu, S., “A Prediction Method for Heat Transfer During Film Condensation on Horizontal Low Integral-Fin Tubes”, ASME Journal of Heat Transfer,1987, Vol. 109, pp. 218-225.
13. Webb, R.L., Rudy, T.M., Kedzierski, M.A., “Prediction of The Condensation Coefficient on Horizontal Integral-Fin Tubes”, Journal of Heat Transfer, 1985, Vol. 107, pp. 369-376
14. Briggs, A., Wen, X.L., Rose, J.W., “Accurate Heat Transfer Measurement for Condensation on Horizontal, Integral-Fin Tubes”, Journal of Heat Transfer, 1992, Vol. 114, pp. 719-726.
15. Honda, H., Takamatsu, H., Takada, N., Makishi, O., “Condensation of HCFC123 in bundles of horizontal finned tubes: effects of fin geometry and tube arrangement”, Int. J. Refrig., 1996, Vol. 19, No. 1, pp. 1-9.

16. Kern, D.Q., “Mathematical Development of Loading in Horizontal Condensers,”, AIChE Journal, 1958, Vol. 4, pp. 157-160.
17. Butterworth, D. “Inundation Without Vapor Shear”, “In Power Condensers Heat Transfer Technology”, 1981, eds. Marto, P.J. and Nunn, R.H., pp. 271-278
18. Grant, I.D.R., Osment, B.D.J., “The Effect of Condensate Drainage on Condenser Performance”,1968, NEL Report no. 350.
19. Honda, H., Nozu, S., “A Generalized Prediction Method For Heat Transfer During Film Condensation On A Horizontal Low Finned Tube”, Proc. 2nd ASME –JSME Thermal Engineering Joint Conference, P.J. Marto and I. Tanasawa, eds., JSME Vol.4, pp. 385-392.
20. Honda, H., Nozu, S., Takeda, Y., “A Theoretical Model of Film Condensation in a Bundle of Horizontal Low Finned Tubes”, Journal of Heat Transfer, 1989, Vol.111, pp. 525-532.
21. Katz, D.L., Geist, J.M., “Condensation on Six Finned Tubes in a Vertical Row”, Trans. ASME, 1948, Vol. 70, pp. 907-914.
22. Taborek, J., “Shell and tube heat exchangers: single phase flow”, Heat Exchanger Design Handbook.

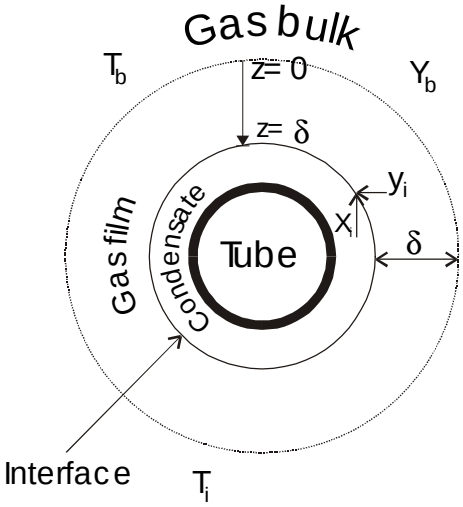

Figure 1: Diagram of condensation process around a condenser tube.

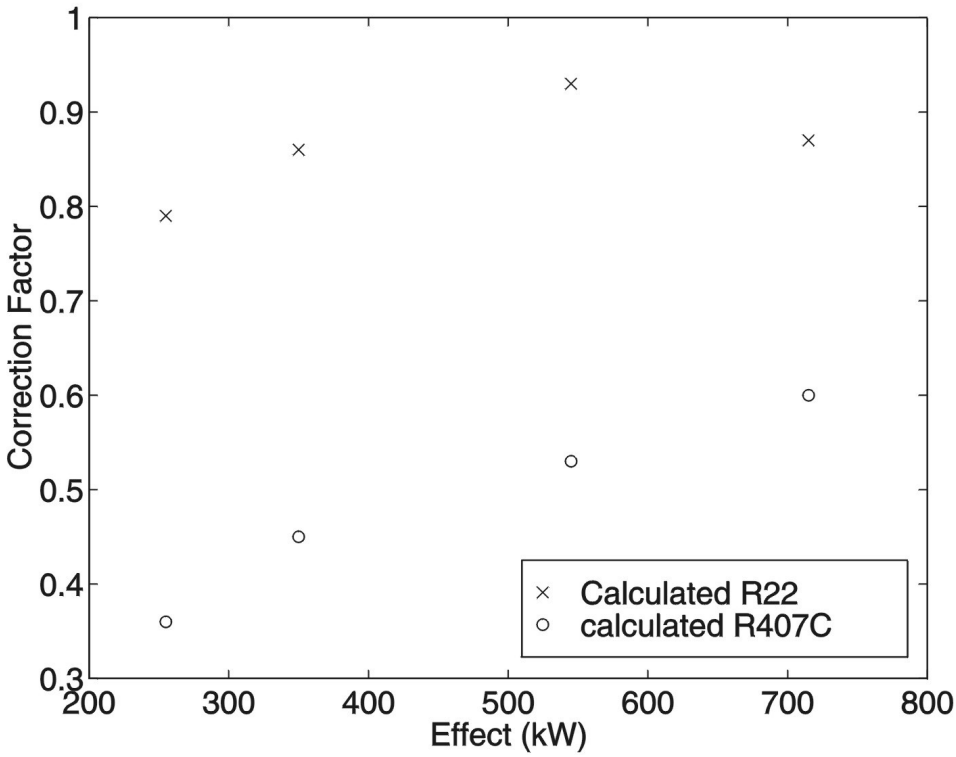

Figure 2: Variation of correction factors for R22 and R407C for the experimental cases presented in [1].

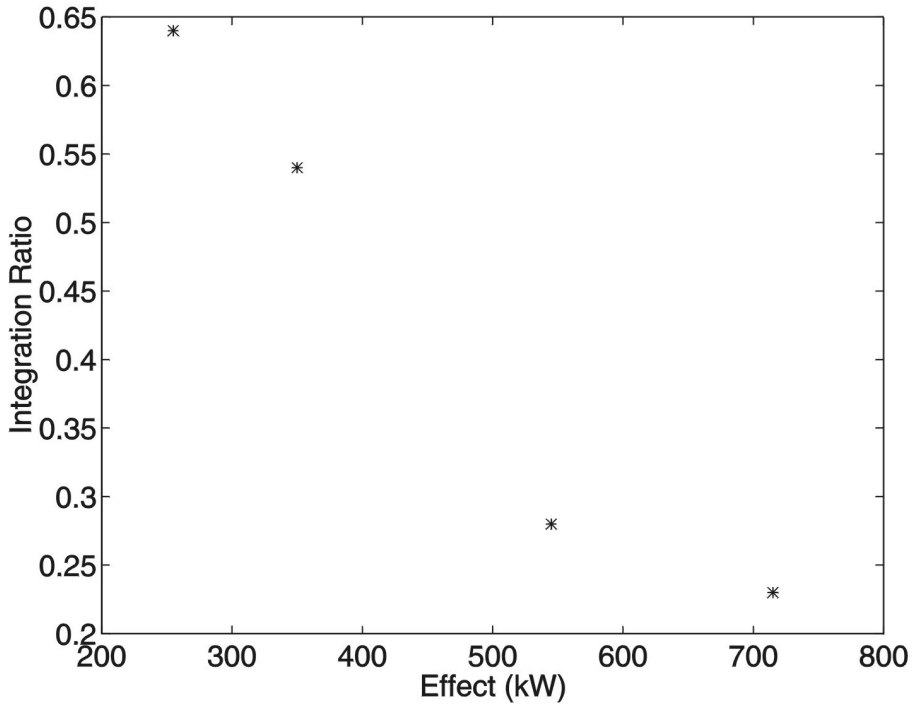

Figure 3: Integration ratio (degree of mixing in the condensate layer) needed to get the correction factor for R407C equal to that of R22 for the experimental cases presented in [1].

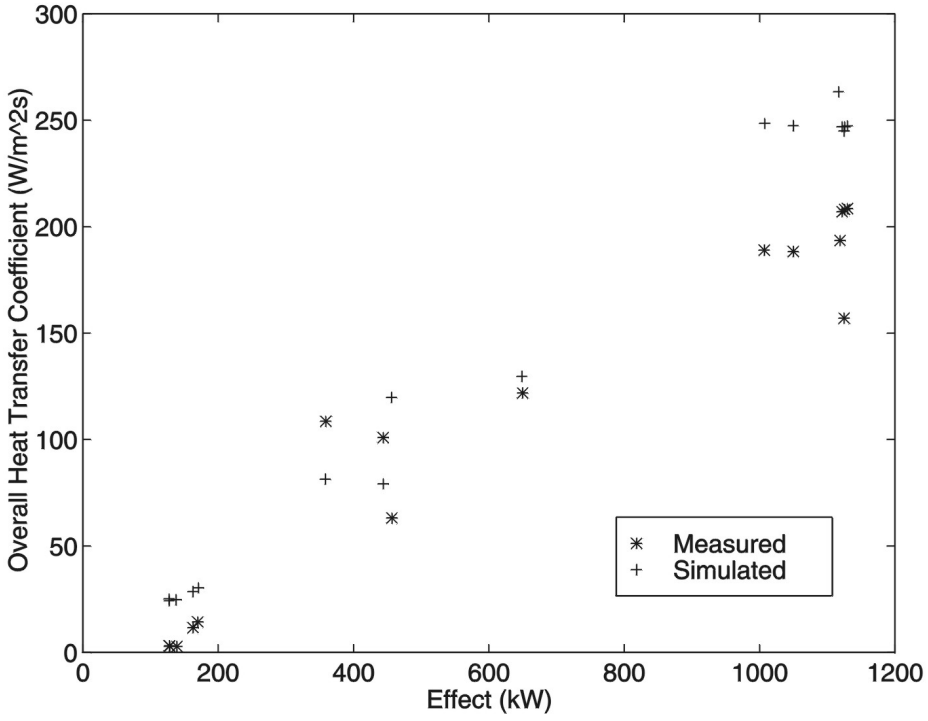

Figure 4: Calculated and experimental overall heat transfer coefficients against the total condenser effect (Q) for R407C.

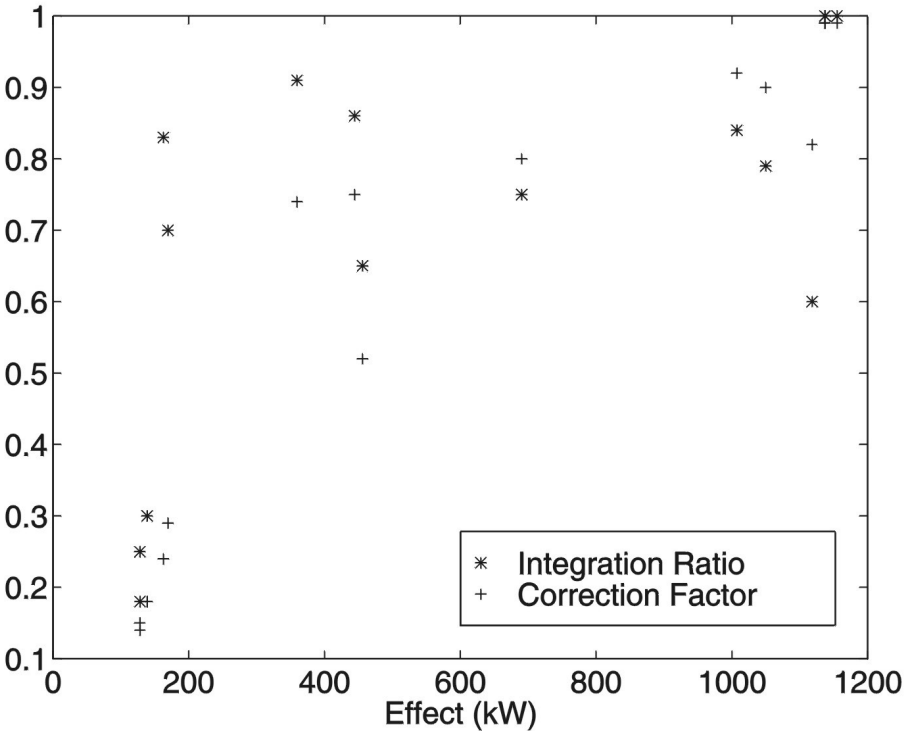

Figure 5: Variation of correction factor and integration ratio (degree of mixing) against condenser effect.